Degradation Kinetics of (±)-4′-Ethyl-2-methyl-3-(1-pyrrolidinyl)propiophenone Hydrochloride (HY-770) and Structure–Stability Relationship among Its Analogues in Aqueous Solution

OSAMU NAGATA‡, TETSUYA TERASAKI*, ETSUKO YADA*, HITOSHI SATO*, IKUMI TAMAI*, AND AKIRA TSUJI*×

Received March 3, 1988, from the *Faculty of Pharmaceutical Sciences, Kanazawa University, Takara-machi, Kanazawa 920, and ‡Central Research Laboratory, Hokuriku Seiyaku Company, Ltd., Katsuyama, Fukui 911, Japan. Accepted for publication August 22, 1988.

Abstract □ The kinetics and pathways for degradation of (±)-4′-ethyl-2-methyl-3-(1-pyrrolidinyl)propiophenone hydrochloride (HY-770; **1**), a newly developed muscle-relaxing agent, and its analogues were studied in aqueous solution at 50 °C, ionic strength 0.5 M, and pH 8.0–12.0. Compound **1** and its four analogues followed pseudo-first-order degradation kinetics at constant pH and temperature. From the analysis of the pH degradation–rate profiles, it is evident that specific hydroxide ion-catalyzed degradations of ionized and un-ionized species occur for **1** and its structural analogue, 3′-fluoro-2-methyl-3-(1-pyrrolidinyl)propiophenone hydrochloride (HN-961; **5**). The hydroxide ion-catalyzed degradation of the ionized species was found to be 100 times faster than that of the un-ionized species and to be the major process at pH <9.0. On the contrary, **1** was extremely stable in 0.5 M HCl at 50 °C, suggesting that the hydronium ion-catalyzed degradation and the spontaneous degradation of the ionized species is negligible. The Arrhenius plot for the degradation of **1** at 35–50 °C and pH 9.0 showed that the apparent energy of activation was 22.0 kcal/mol. The degradation rates of the five structural analogues were significantly dependent on the electron withdrawing effect of the benzene substituents of the molecule.

(±)-4′-Ethyl-2-methyl-3-(1-pyrrolidinyl)propiophenone hydrochloride (HY-770; **1**; Table I) is an orally active and newly developed muscle relaxing agent[1] with a chemical structure similar to that of tolperisone. The pharmaceutical importance of the in vitro stability of **1** prompted us to study the degradation kinetics of this compound and its structural analogues in aqueous solution; this has never been reported elsewhere.

The objectives of the present study were to determine quantitatively the stability of **1** and its analogues under various conditions of solution pH and temperature, and to assess the electron-withdrawing effects of the benzene substituents on the reactivity of these compounds to provide insight into the structure–stability relationship among 2-methyl-3-aminopropiophenone derivatives.

Experimental Section

Chemicals—(±)-4′-Ethyl-2-methyl-3-(1-pyrrolidinyl)propiophenone hydrochloride (HY-770, **1**), 4′-ethyl-2-methylacrylophenone (**2**), 4′-ethylpropiophenone (**3**), HN-961(**5**), HN-1105 (**6**), HN-1081 (**7**), and HN-922 (**8**) were synthetized in the Central Research Laboratory, Hokuriku Seiyaku (Fukui, Japan). The chemical structures of the compounds are listed in Table I. All other chemicals were of reagent grade from Wako Pure Chemical Industries (Osaka, Japan) and were used without further purification.

Kinetic Procedures—An accurately weighed compound was dissolved in 0.5 M KCl solution or borate buffer solution of which the total buffer concentration was varied from 0.05 to 0.20 M. The ionic strength of the buffer was adjusted to 0.5 M by addition of potassium chloride. The initial concentration of the compound was 0.1 mM unless otherwise mentioned. The pH of the solution was maintained at the desired value with 0.05–0.5 M KOH by means of a pH meter (TTT2 titrator, Radiometer, Copenhagen, Denmark) and a pH-stat (TTT2 titrator and ABU12b autoburet, Radiometer) during the period of the stability experiment. Samples were withdrawn at suitable time intervals, cooled on an ice bath, and diluted with an equal volume of 0.1 M HCl to prevent possible degradation during the analysis. The concentration of residual compounds was analyzed by a high-performance liquid chromatographic (HPLC) method.

Analytical Procedures—The liquid chromatograph (BIP-I, Japan Spectroscopic, Tokyo, Japan) was equipped with an ultraviolet (UV) detector (UVIDEC-100-III, Japan Spectroscopic) set at 258 nm, and a 3.9 × 300-mm stainless steel reversed-phase column packed in this laboratory with octadecyl-silane chemically bonded on totally porous silica gel (μBondapak C_{18}, Waters Associates, Milford, MA). The mobile phase was methanol:acetonitrile:60 mM ammonium acetate (3:2:1, v/v). In a separate experiment in which the disappearance of **1** and the formation of its degradation products were simultaneously determined, a step gradient was utilized for the HPLC separation of these compounds as follows: methanol:acetonitrile:21 mM ammonium acetate (23:30:47, v/v) at 0–19 min, and methanol:acetonitrile:60 mM ammonium acetate (3:2:1, v/v) at 19–35 min. The sample (10–60 μL) was injected into the HPLC system and detected at an appropriate AUFS range of 0.01 to 0.32. The chromatography was performed at room temperature, and the samples were eluted at a flow rate of 1.0 mL/min. The mobile phase used and the retention time for each compound are listed in Table I. Peak areas recorded with an integrator (model Chromatopac C-R3A, Shimadzu, Kyoto, Japan) were used to quantitate the concentration of each compound.

pK_a Determination—The apparent pK_a values of **1** and **5** were determined potentiometrically using their HCl salts at an ionic strength (μ) of 0.5 M and at 50 °C.[2] Briefly, a solution containing **1** or **5** (2 mM) and various proportions of ethanol to completely dissolve the drug was titrated with 0.1 M potassium hydroxide at 50 °C. The ionic strength of each solution was adjusted to 0.5 M with potassium chloride.

Results and Discussion

High-Performance Liquid Chromatograms—Typical chromatograms of **1**, **2**, **3**, 4′-ethyl-3-hydroxy-2-methylacrylophenone (**4**), and **5** are presented in Figure 1. The three peaks in panel C represent the major degradation products of **1** after a 4-h reaction at pH 9.0, 50 °C, and μ = 0.5 M. These degradation products were identified by the authentic standard samples of **2** and **3**, as shown in panel A. The chemical structure of **4** was assigned by gas chromatographic-mass spectrometric analysis of itself and its trimethyl silyl derivative. In panel C of Figure 1, the broad peak which appeared just before the peak of **1** was not associated with a degrada-

0022-3549/89/0100-0057$01.00/0

Table I—List of Structures, Sigma Values, and HPLC Conditions for (±)-4′-Ethyl-2-methyl-3-(1-pyrrolidinyl)propiophenone Hydrochloride (HY-770; 1) and Its Analogues

Compound	Structure	σ[a]	Mobile phase MeOH:CH_3CN:$AcONH_4$	Retention Time, min
HN-961 (5)	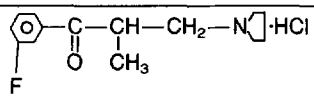	0.34	3:2:1	8
HN-1105 (6)	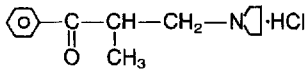	0	3:2:1	10
HN-1081 (7)	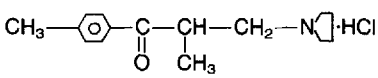	−0.17	3:2:1	11
HY-770 (1)	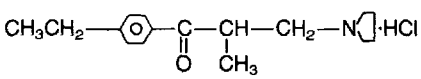	−0.15	3:2:1	11
HN-922 (8)	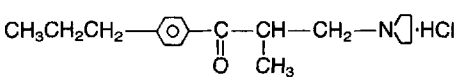	−0.13	3:2:1	14
2	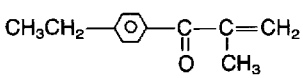	—	23:30:47	17
3	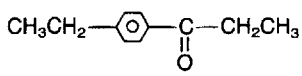	—	23:30:47	14
4	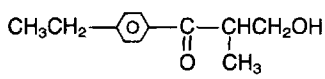	—	23:30:47	7

[a] References 5 and 6.

tion product of 1, but was caused by the step gradient of the organic solvent in the mobile phase. Calibration curves for 1–3 showed good linearity between the concentration and the peak area, with a correlation coefficient of >0.99.

Degradation Pathway—Judging from the change in the chromatograms for the reaction solution, the degradation of 1 may proceed as depicted in Scheme I. Figure 2 shows the time courses of molar concentration of 1–3 during the degradation of 1 (1.0 mM) at 50 °C, pH 9.0, and μ = 0.5 M. By solving the differential equations for 1–3 according to Scheme I, the molar concentration of each compound can be described as follows:

$$[1] = [1]_0 e^{-(k_1 + k_3)t} \quad (1)$$

$$[2] = [1]_0 k_1/(-k_1 + k_2 - k_3)[e^{-(k_1 + k_3)t} - e^{-k_2 t}] \quad (2)$$

$$[3] = [1]_0 k_3/(-k_1 - k_3 + k_4)[e^{-(k_1 + k_3)t} - e^{-k_4 t}] \quad (3)$$

In order to evaluate the values of k_2 and k_4 (i.e., the rate constants for the degradation of 2 and 3), 2 and 3 were separately degraded under the same conditions (the results are shown in Figure 2). In this case, their concentrations can be described as follows:

$$[2] = [2]_0 e^{-k_2 t} \quad (4)$$

$$[3] = [3]_0 e^{-k_4 t} \quad (5)$$

The degradation pathway from 2 and 3 was supposed to be negligible because 3 was not detected during the degradation of 2. The rate constants k_1, k_2, k_3, and k_4 were determined to be 0.516, 0.634, 0.00614, and 0.657 h^{-1}, respectively, by fitting the observed data in Figure 2 to eqs 1–5 by a nonlinear least-squares regression analysis (MULTI).[3] Therefore, it was indicated that the major degradation pathway for 1 under these conditions is the formation of 2 (98.8%). Moreover, 4 would be a possible degradation product of 2 since 4 was also found during the degradation of 2 at pH 9.0 and 50 °C. However, the structure of degradation product of 3 was not assigned, since only a slight amount was produced during the degradation of 1.

Reaction Order and Observed Rate Constants—The kinetics of the degradation of 1 was studied by following the disappearance of the unchanged compound as a function of time. The results indicate that in aqueous solutions, the degradation of 0.1 mM 1 followed pseudo-first-order kinetics with respect to 1 under the constant conditions of pH, temperature, and ionic strength.

Figures 3 and 4 show typical semilogarithmic plots of the residual percent versus time at 50 °C, μ = 0.5 M, and at various pH conditions of 8.0–12.0 and 8.0–11.5 for 1 and 5, respectively. The pseudo-first-order rate constants (k_{pH}) were determined from the slopes of semilogarithmic plots by a least-squares regression analysis and are listed in Table II. The degradation of 1 was apparently concentration independent because the k_{pH} values obtained at 0.1 and 1.0 mM concentrations of 1 were close, as seen in Table II. Thus, second-order degradation was negligible under the present experimental conditions.

On the other hand, no significant degradation of 1 in 0.5 M HCl at 50 °C occurred during the 16-d reaction (<0.5%), indicating the extreme stability of 1 at acidic pH. Hence, the specific hydronium ion-catalyzed degradation and the water-catalyzed spontaneous degradation of the ionized species of 1 was negligible.

General Acid-Base Catalysis—Table III presents the catalytic effect of the borate buffer species on the degradation of 1 over the buffer concentration range 0.05–0.20 M at pH 8.0, 8.5, and 9.5. The results show that the observed first-order rate constants increased linearly with an increase of the buffer concentration at a constant pH. The k_{pH} values were

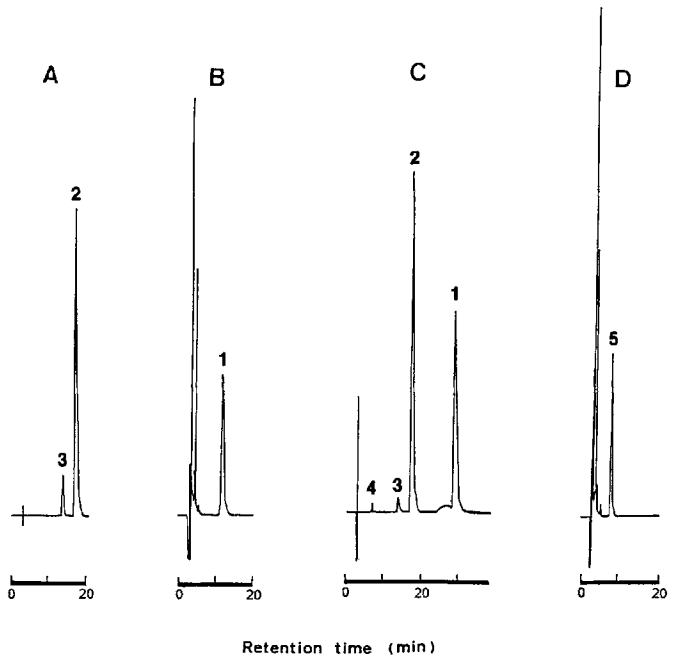

Figure 1—*The HPLC separation of* **1**, *degradation products [i.e., 4'-ethyl-2-methylacrylophenone* (**2**) *and 4'-ethylpropiophenone* (**3**)], *4'-ethyl-3-hydroxy-2-methylpropiophenone* (**4**), *and HN-961* (**5**). *The HPLC conditions are described in the text.* (A) *The HPLC separation of authentic standard* **2** *(0.2 mM) and* **3** *(0.015 mM). The AUFS was 0.32 and the sample volume was 60 μL.* (B) *Typical chromatogram for the degradation of* **1** (AUFS, 0.01; sample volume, 10 *μL). Shown is a 30% degradation of* **1** *(initial conc. 0.1 mM) in aqueous solution at pH 9.0, 50 °C, and ionic strength 0.5 M.* (C) *Typical chromatogram for the degradation of* **1** *and formation of* **2** *and* **3** *(AUFS, 0.32; sample volume, 60 μL). Shown is a 90% degradation of* **1** *(initial conc. 1.0 mM) in aqueous solution at pH 9.0, 50 °C, and ionic strength 0.5 M.* (D) *Typical chromatogram for the degradation of* **5** *(AUFS, 0.01; sample volume, 10 μL). Shown is a 80% degradation of* **5** *(initial conc., 0.1 mM) in aqueous solution at pH 9.0, 50 °C and ionic strength 0.5 M.*

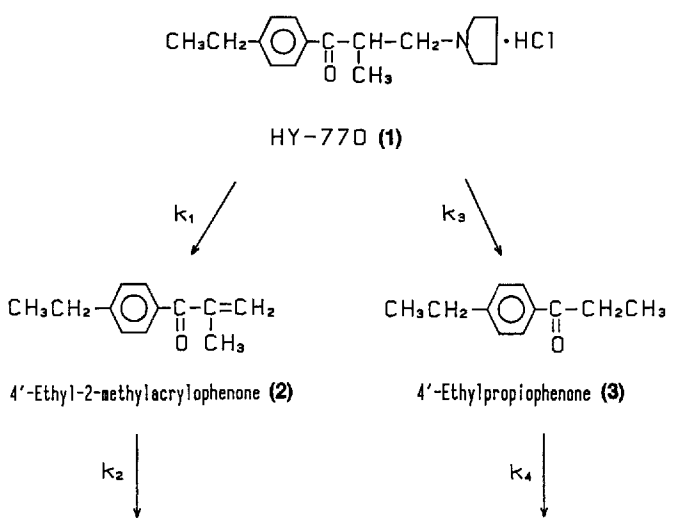

Scheme I—*Degradation pathways of* **1** *(HY-770) in aqueous solution.*

determined by the extrapolation to zero buffer concentration using linear least-squares regression analysis, and are listed in Table III. A fairly good coincidence was observed between the k_{pH} values determined by the pH-stat method (Table II) and those from the borate buffer effect (Table III).

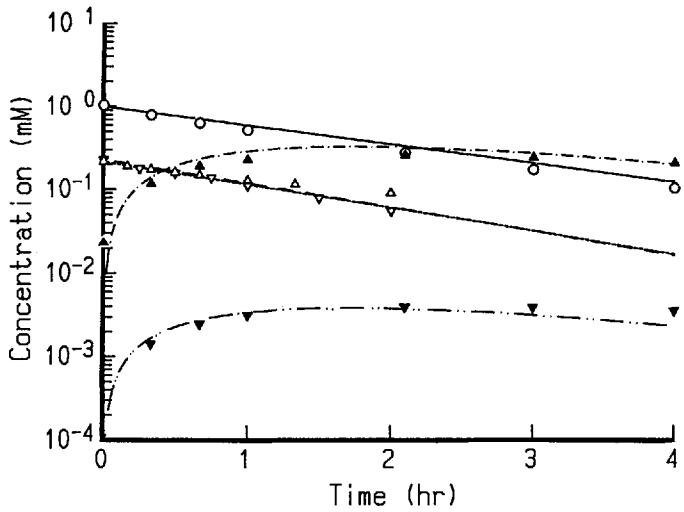

Figure 2—*Concentration–time profile for the disappearance of* **1** (○) *and formation of the degradation products of 4'-ethyl-2-methylacrylophenone,* **2** (▲) *and 4'-ethylpropiophenone,* **3** (▼) *in the degradation of* **1** *and disappearance of* **2** (△) *and* **3** (▽) *in the degradation of* **2** *and* **3**, *respectively. Degradation experiments were carried out at pH 9.0, 50 °C, and ionic strength of 0.5 M. The initial concentrations of* **1**, **2**, *and* **3** *were 1.0, 0.25, and 0.25 mM, respectively. The symbols present the observed values, and the lines are computer-generated simulation curves for the concentrations of these compounds based on eqs 1–5.*

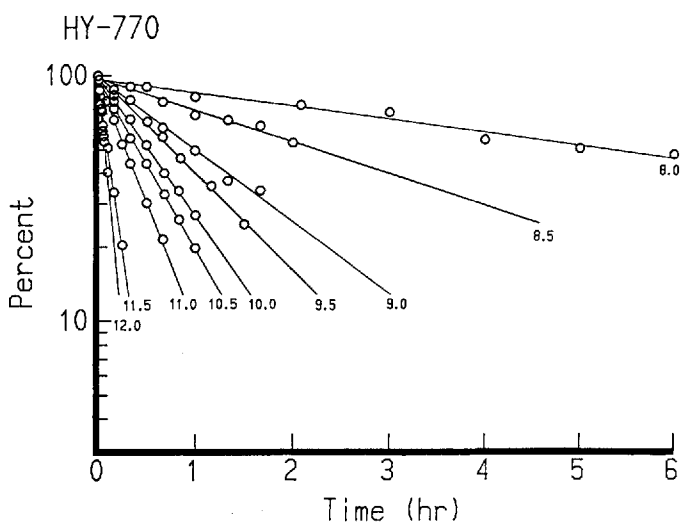

Figure 3—*Typical first-order plots for the degradation of* **1** *(HY-770) in 0.5 M KCl at various pH values, 50 °C, and ionic strength of 0.5 M. The values next to the lines are the pH values of the reaction solutions which were maintained by a pH-stat. The data are normalized to a value of 100 at time zero. The initial concentration of* **1** *was 0.1 mM. Each point represents the observed value, and the solid lines were drawn by linear least-squares regression analysis.*

pK_a Determination—Because it was difficult to dissolve **1** and **5** at 2 mM in the basic solution, ethanol was added to the solution in the pK_a determination. The potentiometrical pK_a value in aqueous solution was estimated from extrapolation of the apparent pK_a values to zero ethanol concentration by linear least-squares regression analysis. As shown in Figure 5, the pK_a values of 9.18 and 9.04 were obtained for **1** and **5**, respectively, at 50 °C and μ = 0.5 M.

pH–Rate Profile—The pH dependency of the pseudo-first-order rate constant (k_{pH}) of **1** degradation over the pH range 8.0–12.0 is illustrated in Figure 6. The log k_{pH}–pH profile for

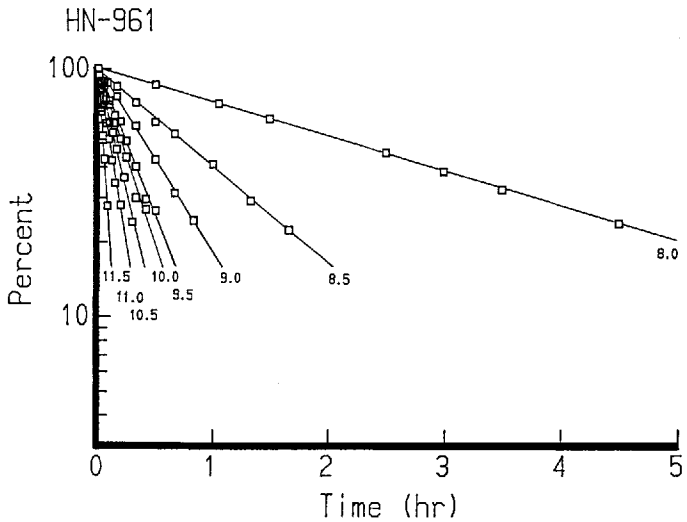

Figure 4—*Typical first-order plots for the degradation of* **5** *(HN-961) in 0.5 M KCl at various pH values, 50 °C, and ionic strength of 0.5 M. The values next to the lines are the pH values of the reaction solution which were maintained by a pH-stat. The data are normalized to a value of 100 at time zero. The initial concentration of* **5** *was 0.1 mM. Each point represents the observed value, and the solid lines were drawn by linear least-squares regression analysis.*

Table II—Effect of Temperature and pH on the Pseudo-First-Order Degradation Rate Constants for (±)-4′-Ethyl-2-methyl-3-(1-pyrrolidinyl)propiophenone Hydrochloride (HY-770; 1) and Its Structure Analogues[a]

Compound	Temperature, °C	pH	k_{pH}, h^{-1}
HY-770 (**1**)	50	8.0	0.127
		8.5	0.301
		10.0	1.30
		10.5	1.60
		11.0	2.29
		11.5	6.06
		12.0	16.3
	35	9.0	0.110
	37	9.0	0.130
	40	9.0	0.220
	45	9.0	0.359
	50	9.0	0.603
		9.0	0.566[b]
2	50	9.0	0.426[c]
3	50	9.0	0.696[c]
HN-961 (**5**)	50	8.0	0.328
		8.5	0.903
		9.0	1.73
		10.0	3.30
		10.5	4.57
		11.0	6.62
		11.5	15.5
	35	9.0	0.309
HN-1105 (**6**)	35	9.0	0.160
HN-1081 (**7**)	35	9.0	0.0904
HN-922 (**8**)	35	9.0	0.106

[a] Initial concentration, 0.1 mM. [b] Initial concentration, 1.0 mM. [c] Initial concentration, 0.25 mM.

5 obtained under the same kinetic conditions is also illustrated in Figure 6. The profile for **5** is very similar in shape to that for **1**, but **1** was 2.7 times more stable than **5**. In these log k_{pH}–pH profiles, the shoulder-type breaks are due to the different rates between the reaction of the hydroxide ion-catalyzed degradation of the ionized species of **1** or **5** (reaction

Table III—Effect of Borate Buffer Concentration on the Pseudo-First-Order Degradation Rate Constants for (±)-4′-Ethyl-2-methyl-3-(1-pyrrolidinyl)propiophenone Hydrochloride (HY-770; 1) at 50 °C

pH	k_{obs}, h^{-1}				k_{pH}, h^{-1}
	0.05 M	0.10 M	0.15 M	0.20 M	
8.0	0.171	0.149	0.177	0.235	0.123
8.5	0.335	0.465	0.478	0.464	0.340
9.5	1.03	1.17	1.23	1.26	0.971

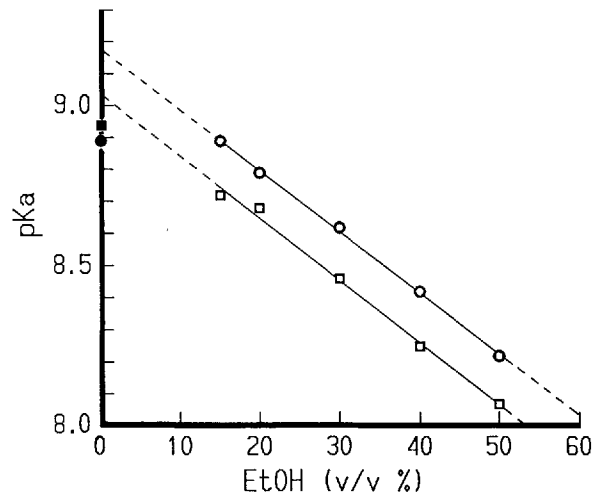

Figure 5—*Plot of apparent pK_a values versus percent ethanol in aqueous solution containing* **1** *(circles) and* **5** *(squares). Open symbols represent the observed value at different percents of ethanol at 50 °C and ionic strength of 0.5 M. The solid lines were drawn by regression of the potentiometrically determined pK_a values at the drug concentration of 2 mM. Closed symbols represent the kinetically determined pK_a value from the analysis of the log k_{pH}–pH profile using eq 6.*

1) and that of un-ionized species of **1** or **5** (reaction 2). Hence, the total shape of the log k_{pH}–pH profile can be described by the following equation:

$$k_{pH} = k_{OH}Kw/a_{H^+}[a_{H^+}/(K_a + a_{H^+})] + k'_{OH}Kw/a_{H^+}[K_a/(K_a + a_{H^+})] \quad (6)$$

where a_{H^+} represents hydrogen activity which was determined from 10^{-pH}, k_{OH} and k'_{OH} represent the second-order catalytic constants for specific hydroxide ion-catalyzed degradation of ionized and un-ionized species of **1** or **5**, respectively, and Kw is the autoprotolytic constant.

Incorporating the value of $Kw = 5.47 \times 10^{-14}$ at 50 °C and μ = 0.5 M,[4] kinetic rate constants (k_{OH} and k'_{OH}) were obtained by use of MULTI, with weighting based on the reciprocal of each k_{pH} value (Table IV). The pK_a values were also obtained as the fitted parameters and are listed in Table IV (designated as kinetically determined pK_a). The pK_a values determined potentiometrically relate to the substrate as a reactant, whereas the kinetically determined value probably relates to the transition state in the degradation reaction. This may account for the very similar kinetically determined pK_a values for **1** (HY-770) and **5** (HN-961) compared with the more disparate values determined potentiometrically. The curves in Figure 6 are the computer-generated simulation curves according to eq 6 using thus obtained kinetic and physiochemical parameters (Table IV). The calculated k_{pH} values are in good agreement with the observed values, indicating that eq 6 could adequately de-

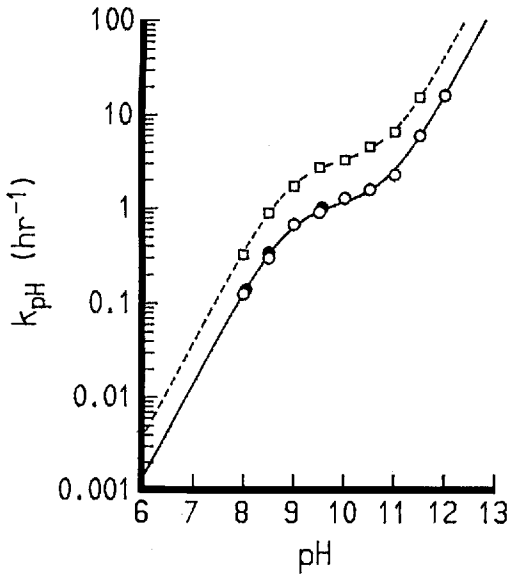

Figure 6—*Log k_{pH}–pH profiles for the degradation of* **1** *and* **5** *at 50 °C and ionic strength of 0.5 M. The lines represent the best-fitting curve calculated according to eq 6 using nonlinear least-squares regression (MULTI) and the rate constants listed in Table IV. The points are the experimental values obtained by a pH-stat for* **1** (○) *and* **5** (□), *or from the study of borate buffer effect which was extrapolated to zero-buffer concentration* (●). *The respective values are listed in Table III.*

Table IV—Degradation Rate Constants and pK_a Values of Compounds 1 (HY-770) and 5 (HN-961) at 50 °C and μ = 0.5 M[a]

Compound	$k_{OH} \times 10^4$, $M^{-1}\cdot h^{-1}$	$k'_{OH} \times 10^2$, $M^{-1}\cdot h^{-1}$	pK_a[b]	pK_a[c]
HY-770 (**1**)	2.58 ± 0.14	2.82 ± 0.09	8.89 ± 0.06	9.18
HN-961 (**5**)	6.90 ± 0.63	6.98 ± 0.23	8.94 ± 0.05	9.04

[a] Values are expressed as the mean ± SD except for the potentiometrically determined pK_a values. [b] Kinetically determined. [c] Potentiometrically determined.

scribe k_{pH} as a function of pH for both **1** and **5**. Accordingly, the hydroxide ion-catalyzed degradation of the un-ionized species is suggested to be predominantly operative at pH values >12.0, and that of ionized species is suggested to be predominant at pH values <9.0.

Effect of Temperature—The temperature dependence of the degradation of **1** was studied in unbuffered solution at pH 9.0 and at μ = 0.5 M using a pH-stat titration technique. The Arrhenius plot is shown in Figure 7. Based on these data, the apparent energy of activation was calculated to be 22.0 kcal/mol, in which the activation energy for the specific hydroxide ion-catalyzed degradation of **1**, and the heats of ionization of water (13.1 kcal/mol)[4] and **1** should be included.

Structure–Stability Relationship—The pseudo-first-order degradation rate constants (k_{pH}) of **6** (HN-1105), **7** (HN-1081), and **8** (HN-922) were also determined at 35 °C and μ = 0.5 M. The solution pH was maintained at 9.0 by a pH-stat. Although the pK_a values would be different among these derivatives, the order of k_{pH} values was **5** > **6** > **1** ≒ **8** ≒ **7**

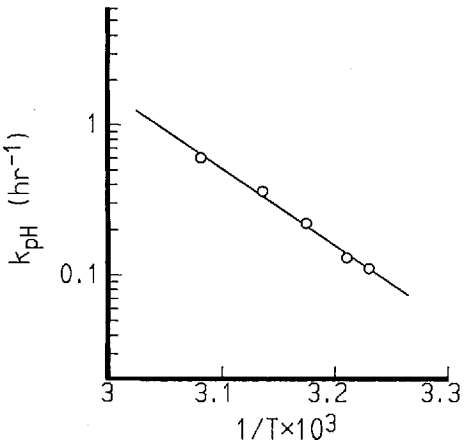

Figure 7—*Arrhenius plot of the pseudo-first-order rate constant (k_{pH}) for the degradation of* **1** *at pH 9.0 in 0.5 M KCl solution. The pH of the reaction solution was maintained by a pH-stat.*

(Table II), and found to be in good agreement with the order of their Hammett σ values,[5,6] which are listed in Table I. Inspection of eq 6 suggests that k_{pH} at pH 9.0 is almost dependent on reaction 1 among the five structural analogues. Consequently, the observed σ–k_{pH} relationship strongly suggests that the reactivity of **1** and its structural analogues are dependent on the electron-withdrawing effect of the benzene substituents, which could accelerate the hydroxide ion-catalyzed hydrogen exclusion from the carbon atom next to the keto group of the ionized species of these analogues. Though the spontaneous degradation of un-ionized species is kinetically equivalent to the hydroxide ion-catalyzed degradation of ionized species, the former reaction may not be a rationale for the hydrogen exclusion from the molecule, as compared with the latter reaction. Accordingly, it follows that the lower the sigma value of the benzene substituent, the more stable could be the 2-methyl-3-aminopropiophenone derivative. This finding will provide useful information concerning the structure–stability relationships of this series of compounds with the aim of increasing its chemical stability.

References and Notes

1. Morikawa, K.; Oshita, M.; Yamazaki, M.; Ohara, N.; Mizutani, F.; Kato, H.; Ito, Y.; Kontani, H.; Koshiura, R. *Arzneim.-Forsch.* **1987**, *37*, 331–336.
2. Albert, A.; Serjeant, E. P. *Determination of Ionization Constants*, 3rd Ed.; Chapman and Hall: London, 1984, Chapter 2–3, pp 14–69.
3. Yamaoka, K.; Tanigawara, Y.; Nakagawa, T.; Uno, T. *J. Pharmacobio-Dyn.* **1981**, *4*, 879–885.
4. Harned, H. S.; Hamer, W. J. *J. Am. Chem. Soc.* **1933**, *55*, 2194–2206.
5. Hansch, C.; Leo, A.; Unger, S. H.; Kim, K.-H.; Nikaitani, D.; Lien, E. J. *J. Med. Chem.* **1973**, *16*, 1207–1216.
6. Hansch, C.; Rockwell, S. D.; Jow, P. Y. C.; Leo, A.; Steller, E. E. *J. Med. Chem.* **1977**, *20*, 304–306.

Acknowledgments

The authors thank Mr. Masaru Nakanishi, Miss Toshiko Sakashita, Masahiro Yamazaki, and Mr. Eiji Takahara for their excellent technical assistance.